6.4

POTENTIAL FORECAST IMPACTS FROM SPACE-BASED LIDAR WINDS: RESULTS FROM A REGIONAL OBSERVING SYSTEM SIMULATION EXPERIMENT

Stephen S. Weygandt[1], Thomas W. Schlatter[1], Steven E. Koch[1], Stanley G. Benjamin[1], Adrian Marroquin[1], John R. Smart[1], Michael Hardesty[2], Barry Rye[2], Aniceto Belmonte[2], Graham Feingold[2], Dale M. Barker[3], Qinghong Zhang[3], Dezso Devenyi[1]

[1] NOAA Research - Forecast Systems Laboratory, Boulder, CO
[2]NOAA Rsearch - Environmental Technology Laboratory, Boulder, CO
[3]National Center for Atmospheric Research, Boulder, CO

1. INTRODUCTION

For at least two decades, there has been strong interest in the possibility of obtaining atmospheric wind measurements from a Doppler lidar profiling system flown aboard a polar orbiting satellite (Baker et al., 1995 and references therein). While the potential benefit to both global and regional weather prediction from the assimilation of these lidar observations into numerical models is significant, the financial burden of deploying a space-based lidar profiling system is large. Therefore, it is prudent to obtain an accurate estimate of the likely forecast improvement from the lidar observations before making a decision regarding deployment.

Carefully constructed observing system simulation experiments (OSSEs; Atlas 1997, Lord et al. 1997) provide the appropriate framework for estimating the likely forecast improvement from a space-based Doppler Wind Lidar (DWL) system. OSSEs begin with a long-duration pure forecast known as a "nature run," conducted with a numerical weather prediction model known to possess an accurate climatology. Using the four-dimensional "truth" atmosphere obtained from the nature run, all conventional observation types can be sampled, as well as those that would be available from the future observing system. A second numerical prediction model (one with different characteristics but similarly accurate climatology is strongly preferred) is then used to assimilate the observations and produce forecasts that can be verified against the nature run. Comparison can then be made of experiments using all the conventional observations (representing the current forecast skill) with experiments including the conventional observations plus the observations from the future observing system.

Prior to making these comparisons, however, it is extremely important to verify that the impact in the OSSE forecast system from denying simulated conventional observations matches that of current real-data forecast systems when actual data from the same observation types is withheld. This validation/calibration procedure helps to establish the credibility of the OSSE and increases the confidence that the forecast improvement foreseen in the OSSE will be realized when the observing system is actually deployed (Lord et al. 1997). In addition to providing a base estimate of forecast improvement from a new observing system, OSSEs allow us to test the effectiveness of variations in system design parameters, scan strategies, and data quality. This is especially important for the DWL, because the technology for obtaining accurate space-based Doppler lidar wind is still being perfected, and more than one type of lidar system and scan strategy have been proposed.

Thus, as a prelude to a possible launch of a DWL system, a number of organizations have collaborated to conduct a series of Observing System Simulation Experiments (OSSEs) to test the forecast impact for various DWL scenarios. One component has been a global OSSE conducted by the National Centers for Environmental Prediction (NCEP), with assistance from a number of other organizations (Lord et al. 2001). Because the DWL platform will provide a wealth of observations over data-sparse oceanic regions, a global OSSE is an especially appropriate framework for evaluating the impact on forecast skill. However, much of the day-to-day operational forecast guidance is provided by regional mesoscale models, which are very different from global models. These

* *Corresponding author address:* Stephen S. Weygandt, NOAA/FSL, R/FS1, 325 Broadway, Boulder, CO 80305, Stephen.Weygandt@noaa.gov

mesoscale model differences include: 1) better resolution of local forcing from surface features, 2) application over data-rich regions, 3) utilization of high-frequency assimilation, and 4) observation impact from both data assimilation and lateral boundary conditions. To address the unique data sensitivity questions pertaining to these mesoscale models, a regional DWL OSSE has been conducted by NOAA's Forecast Systems Laboratory (FSL) with assistance from the NOAA Environmental Technology Laboratory (ETL) and the National Center for Atmospheric Research (NCAR). The goal of the regional OSSE is to estimate the potential value of lidar observations in more detailed forecasts over the continental U.S. (CONUS).

2. REGIONAL OSSE METHODOLOGY

Because the limited-domain mesoscale models used for the regional OSSE require lateral boundary conditions, the global and regional OSSEs are inextricably linked, as illustrated in Fig. 1. The global nature run provides lateral boundary conditions for the regional nature run (RNR), while the global assimilating model provides lateral boundary conditions for the regional assimilating model. On both global and regional scales, nature runs are the source of the simulated observations and provide the "truth" against which the OSSE forecasts are verified.

For the global nature run, a 30-day forecast has been created by the European Centre for Medium-Range Weather Forecasts (ECMWF) for the period from 5 February through 6 March1993. Global assimilation experiments have been completed with the NCEP Global Forecast System (GFS) (Lord et al. 2002). The 11-day RNR simulation was completed using a 10-km version of the MM5 nonhydrostatic model, utilizing a 740 x 520 x 43 point domain covering a large portion of North America and adjacent oceans. Physical parameterizations employed in the RNR included Kain-Fritsch convection, Schultz microphysics, Burk-Thompson turbulence, RRTM radiation, and the Rapid Update Cycle (RUC) land surface model. Initial and boundary conditions are provided by the ECMWF global nature run. Additional details concerning the RNR are given in Marroquin et al. (2001). A detailed examination of the regional nature run was completed by NCAR (Barker and Zhang 2001). Despite some shortcomings in the RNR (drift from the ECMWF nature run, warm bias at low levels), the RNR was found to represent a plausible evolution of the real atmosphere, suitable for producing simulated observations.

A summary of the dates and duration of the various components of the regional OSSE experiment forecasts is presented in Table 1. The RNR pure forecast extends from 0000 UTC 11 February 1993 through 0000 UTC 22 February 1993. Following a 48-h spin-up period, observations were extracted from the RNR beginning at 0000 UTC 13 February 1993. Observation extraction ended at 0000 UTC 20 February 1993, allowing for verification against the nature run of a 48-h forecast from the regional assimilation model. The following types of conventional observations were extracted: rawinsondes, aircraft, wind profilers, radar velocity azimuth display (VAD) wind profiles, surface METARs (meteorological aerodrome reports), and buoys. Because the density of aircraft observations was much less in 1993 than it is today, use of 1993 observation distribution is inappropriate for the OSSE experiment and could lead to an exaggeration of the impact from the lidar observations. It was therefore decided to use an observation distribution from 2001 for the generation of simulated observations. Random errors consistent with those expected for each observation type were then added to the observations as indicated in Table 2.

For the lidar observations, relevant model variables (winds, hydrometeors) were extracted from the RNR at locations corresponding to the predetermined lidar line-of-sight beam paths. These locations were computed by ETL based on specified orbit/scan parameters.

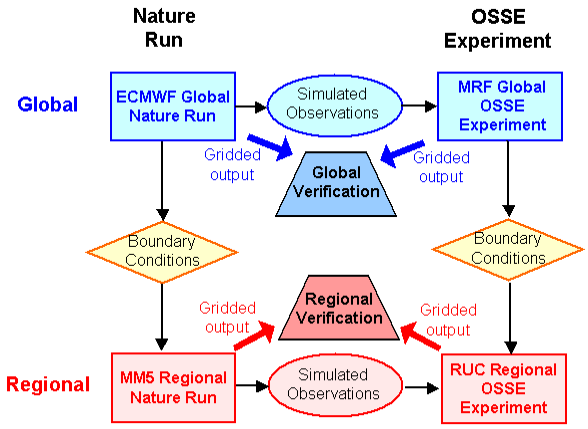

Fig. 1. Principal components of the global and regional OSSE system and their interrelationship. Boundary conditions are supplied by the global nature run and global OSSE experiment to the regional nature run and regional OSSE experiment, respectively. Observations are supplied by the global and regional nature runs to the global and regional OSSE experiments, respectively.

Table 1. Summary of regional OSSE run schedule. All dates are for 1993. Unless noted, all times are 00 UTC.

Dates	Duration	Event
Regional Nature Run		
11-22 Feb	11 days	Regional nature run (pure forecast simulation)
11-13 Feb	2 days	Spin-up
13-20 Feb	7 days	Observation extraction
20-22 Feb	2 days	Verification for last 48-h assimilation forecast
Regional Assimilation Run		
13-20 Feb	7 days	Regional assimilation runs (3-h update cycle, 48-h fcsts at 00, 12 UTC, 18-h fcsts at 06, 18 UTC)
13-15 Feb	2 days	Spin-up (3-h update cycle ongoing)
15-20 Feb	5 days	Generation of 48-h and 18-h fcsts (verified against regional nature run)

Table 2. Observations types simulated from the regional nature run. For each observation type, the fields reported and the standard deviations of added random errors are given. Approximate observation data counts for 1200 and 1500 UTC are also shown.

Observation Type	Fields Reported	Random Error S.D.	Number of reports 12 UTC	15 UTC
Rawinsonde	Height Temp Dew pt Wind spd Wind dir	50.0 m 1.0 K 0.75 K 1.0 m s^{-1} 2.5 deg	3700	0
Profiler/VAD	Wind spd Wind dir	0.5/1.5 m s^{-1} 2.5/3.0 deg	2600	2600
Aircraft	Temp Wind spd Wind dir	1.5 K 1.0 m s^{-1} 2.5 deg	1200	1300
METAR/Buoy	Temp Dew pt Wind spd Wind dir	0.5 K 0.75 K 0.5 m s^{-1} 2.5 deg	1600	1600
Lidar	Radial vel	none	1500	1500

Using this extracted model information, ETL then computed line-of-sight wind observations for the most idealized case (no observation errors, no attenuation due to clouds) and a number of more realistic scenarios (attenuation by ice and water clouds). Consistent with signal-to-noise ratio demands for obtaining realistic lidar observations, a 450-km orbit was assumed for the regional OSSE experiments. An eight-point "step-stare" scan strategy (depicted in Fig. 2) was assumed for these experiments. For each polar orbit satellite swath, this strategy obtains vertical profiles of observations for two look angles along four parallel paths. Additional details concerning the simulation of the DWL data are provided in Feingold et al. (2002).

During each 24-h period, the polar orbiting satellite completes six sweeps across the RUC

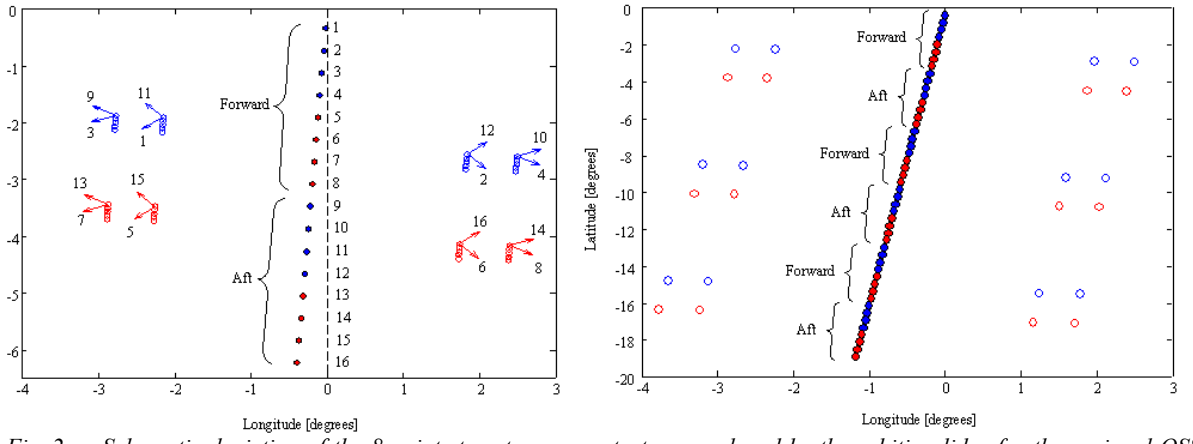

Fig. 2. Schematic depiction of the 8-point step-stare scan strategy employed by the orbiting lidar for the regional OSSE experiments. Using eight fore beam-shots and eight aft beam-shots, two stares from different angles are obtained at each of eight points, yielding a swath of four rows of observations.

CONUS domain. The approximate observation counts for all platforms for 1200 UTC (a rawinsonde time) and 1500 UTC (a non-rawinsonde time) are given in Table 2, along with the analysis variables provided by each platform. These numbers illustrate the volume of current observation data that the lidar winds must compete against to influence the analyses and subsequent forecasts. The distinction between the rawinsonde times (0000, 1200 UTC) and the non-rawinsonde times (all other times) is crucial, as much less information is provided by the current observations at the non-rawinsonde times. Thus we would expect a greater impact from the lidar observations for forecasts initialized at non-rawinsonde times. Recognizing that the current platforms provide two components of the horizontal wind (U and V) compared with the single component (V_r) provided by the lidar, we can see that at rawinsonde times the lidar will provide about 8% more wind component observations, while at non-rawinsonde times the lidar will provide about 15% more wind component observations.

For the regional assimilation experiments, a 40-km 3-h cycle version of the RUC 20-km 1-h model/assimilation system (Benjamin et al. 2003a,b) was used. The RUC model utilizes a unique vertical coordinate system, in which a smooth transition is made between isentropic levels defined in the free-atmosphere and sigma-pressure levels near the ground. RUC model components include the Grell-Devenyi ensemble cumulus parameterization (Grell and Devenyi, 2002), the Smirnova land surface model (Smirnova et al. 2000) and the NCAR five-class microphysics scheme. The 151 x 113 x 50 point CONUS RUC model domain covers a smaller area than the RNR. The RUC assimilation cycle commenced at 0000 UTC 13 February 1993 and continued through 0000 UTC 20 February 1993. For this application, the RUC 3DVAR analysis (Devenyi and Benjamin 2003) was modified to accommodate plane polar radial velocities, and was used to provide 3-hourly analysis updates. Within each analysis update, all observations within a 90-minute observation window were assimilated. At the 0000 and 1200 UTC (rawinsonde) initialization times 48-h forecasts were completed, while 18-h forecast were completed at the 0600 and 1800 UTC (non-rawinsonde) initialization times. Following a 48-h spin-up period of the regional assimilation cycle, verification statistics were collected over a five-day period (see Table 1). This results in eleven 48-h forecasts from rawinsonde initialization times and twelve 18-h forecasts from non-rawinsonde initialization times.

3. REGIONAL OSSE CALIBRATION

Although the use of a 2001 observation distribution is crucial for accurately representing the present mix of observations, it precludes application of a detailed validation/calibration procedure such as that applied to the global DWL OSSE (Masutani et al. 2002). This is because no real observations corresponding to the 2001 distribution are available for the 1993 case. We have, therefore, pursued a simpler, two-track approach to verifying the realism of the OSSE system error characteristics. First, we have compared the bias and standard deviation errors for wind, moisture, temperature and height forecasts between an OSSE assimilation cycle using all conventional observations and an operational version of the RUC model using similar sets of observations (not shown). With minor exceptions, good agreement was found in both the error growth with time and the distribution of errors with height. One exception was a low-level cold bias in the OSSE cycle compared to the RNR (that exceeded the corresponding bias in a comparison of real-data forecasts against actual observations). This bias appears to be related to an inadequate snow cover initialization in the RNR.

As a second method for verifying the realism of the OSSE system, we compared the data impact statistics between OSSE experiments using simulated conventional observations and a real-data observing system experiment (OSE) conducted for a different period (4-16 February 2001). For these and all subsequent observation impact comparisons, we normalize the forecast impact by computing a percentage forecast improvement relative to the control forecast (which used only the conventional observations) as follows:

$$\%\ improvement = \frac{CNTL - EXP}{CNTL}$$

where CNTL is the control error and EXP is the experiment error. Positive (negative) values indicate improved (worsened) forecast skill. For winds the error is a vector root mean square (rms) error and for all other variables the error is a standard deviation (std. dev.) error. Fig. 3 shows a vertical profile of the percent improvement from denying aircraft observations for both the simulated-data OSSE forecasts and the Feb 2001 real-data test period. The percentage improvements (negative, indicating a worse forecast without the aircraft observations) are quite similar below 300 hPa for the simulated and real-data cases.

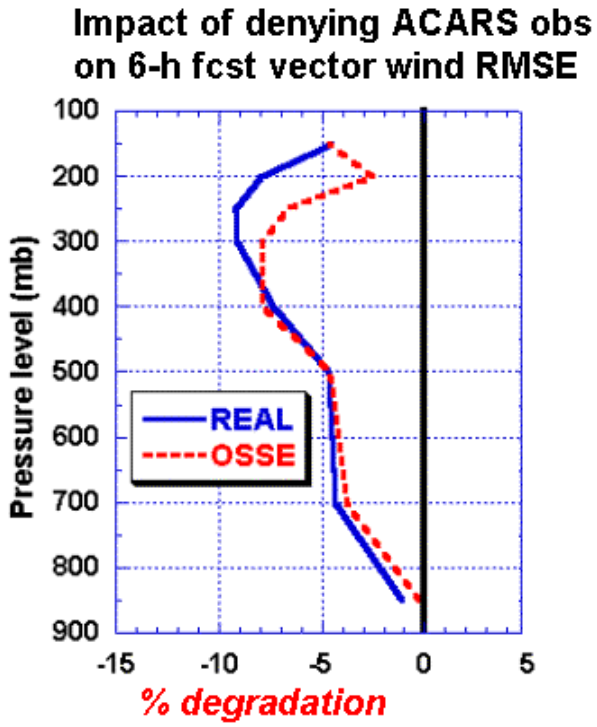

Fig. 3. Comparison of real-data and OSSE (simulated-data) vertical profiles of percent degradation for 6-h vector wind forecasts due to the denial of aircraft data. Negative values shown indicate larger rms errors when the aircraft observations are removed. For the real data case, point verification is performed against the CONUS rawinsonde network. For the OSSE case, grid verification is performed over a region covering the CONUS rawinsonde network.

The differences above 300 hPa have been traced back to a weakening of the upper-level winds (and resultant lessening of the error) in both the RNR and OSSE cycles compared to the Feb 2001 real-data case. This appears to be related to differences in the dominant weather regimes between the two cases. During the OSSE period (15-22 Feb. 1993) the weather was generally very cold over the CONUS RUC domain with a low tropopause; for the real-data period (4-16 Feb. 2001) the weather was very mild with a high tropopause. Additional data denial comparisons are planned to further verify the realism of the OSSE system. The basic conclusion, however, is that with some modest explainable exceptions, the OSSE system adequately mimics the data impact characteristics of a real-data system.

4. REGIONAL OSSE RESULTS

As noted in Section 1, lidar observations will affect a regional model forecast through two paths: 1) the direct assimilation of the observations within the regional assimilation cycle and 2) the use of lateral boundary conditions from a larger model which also assimilates lidar observations. We have examined the impacts from each path independently, as well as the combined impact. We have further stratified the results by initialization time (rawinsonde vs. non-rawinsonde), consistent with the expected difference in forecast impact for these two classes.

Table 3. Summary of idealized lidar experiments

Experiment Name	Obs Assim in Boundary Conditions	Obs Assim in Regional Cycle
CnvCnv	Conventional	Conventional
CnvLid	Conventional	Conventional + Lidar
LidCnv	Conventional + Lidar	Conventional
LidLid	Conventional + Lidar	Conventional + Lidar

A subset of the experiments completed to date is described here, and summarized in Table 3. It is important to note that these experiments represent upper bounds on potential forecast impact, as we have assumed perfect lidar observations (no errors added) and maximal coverage (no loss of lidar observations due to clouds). In the first experiment (CnvCnv), only conventional observations were used in the regional assimilation and in the global experiment, which supplied the lateral boundary conditions. This experiment represents the present state-of-the-art for the regional assimilation system and serves as a control against which the other experiments are compared. In the second experiment (CnvLid), the boundary conditions are the same (reflecting only the conventional observations), but idealized lidar observations are added to the regional assimilation cycle. Fig. 4 shows the time evolution of the percent improvement of the rms wind forecast errors from the addition of the lidar observations, stratified by initialization time (0000 and 1200 UTC rawinsonde initialization times vs. 0600 and 1800 UTC non-rawinsonde initialization times). As can be seen, the addition of the lidar observations results in a modest forecast improvement, and as expected, the improvement is greater for the non-rawinsonde

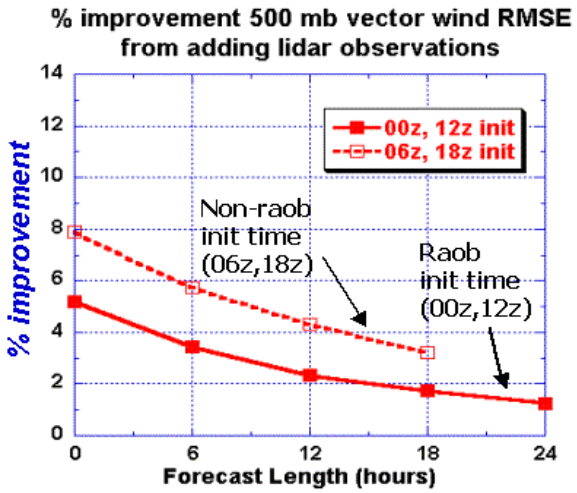

Fig. 4. Time series of percent improvement for 500 mb vector wind forecasts due to the assimilation of idealized lidar observations (on the regional domain) at rawinsonde and non-rawinsonde initialization times. Positive values shown indicate smaller rms errors when the lidar observations are added.

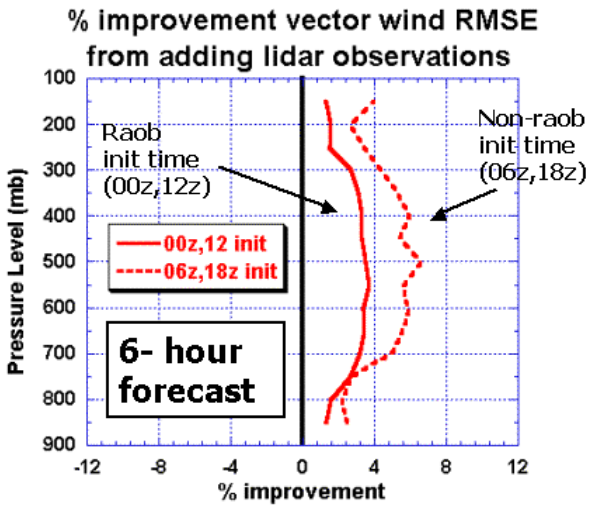

Fig. 5. Vertical profiles of percent improvement for 6-h vector wind forecasts due to the assimilation of lidar observations (on the regional domain) for rawinsonde and non-rawinsonde initialization times. Positive values shown indicate smaller rms errors when the lidar observations are added.

initialization times, when the lidar observations are competing with fewer conventional observations. Also anticipated is the decrease in forecast impact with time, as the lateral boundary conditions (containing only conventional observation data) sweep information in from the boundaries. Examination of the percent improvement for other fields (temperature, moisture, geopotential) indicates small but positive impacts from the addition of the lidar observations.

The vertical distribution of the percent improvement in the 6-h forecast is presented in Fig. 5, and again shows a larger improvement for the non-rawinsonde initialization times. Especially evident is the significantly larger percent improvement in the mid- and upper-troposphere wind forecasts compared to the boundary layer (where the lidar observations are competing with hundreds of surface observations). The consistent forecast improvement throughout the depth of the atmosphere even for rawinsonde initialization times is especially encouraging.

The results from the experiment in which lidar observations affect the regional assimilation through only the lateral boundary conditions (LidCnv, not shown) also show a forecast improvement. For this case, however, the percent improvement increases with time, reaching a maximum of near 10% for the non-rawinsonde 18-h forecasts and near 9% for the rawinsonde 48-h forecasts. The forecast improvement for vector winds from the combined effects of lidar observations in both the lateral boundary conditions and the regional data assimilation (experiment LidLid) are shown in Fig. 6. Comparison of this combined impact with the individual contributions (not shown) indicates that the boundary condition and assimilation impacts are nearly additive.

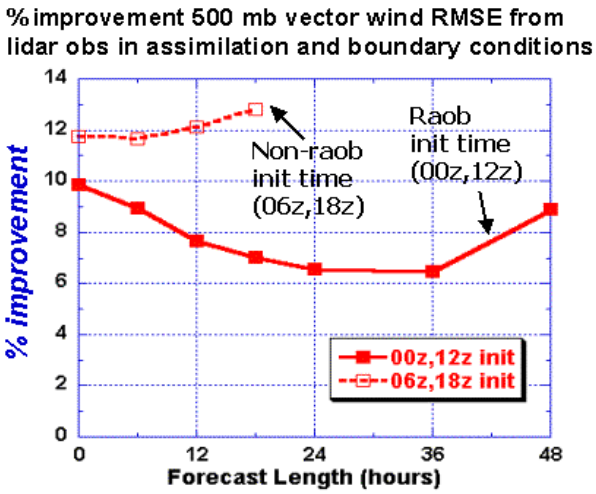

Fig. 6. Time series of percent improvement for 500 mb vector wind forecasts from combining assimilation of idealized lidar observations on the regional domain with the use of idealized lidar observations in the lateral boundary conditions (shown for rawinsonde and non-awinsonde initialization times). Positive values shown indicate smaller rms errors when the lidar observations are utilized.

For the non-rawinsonde initialization times, the combined percent improvement is nearly constant at 12%. For the rawinsonde initialization time, the combined percent improvement decreases from near 10% at the analysis time to near 6% at 36-h, then increases to near 9% at 48-h.

In addition to improving wind forecasts, the use of lidar observations (in both the regional assimilation and boundary conditions) yields modest improvements in the temperature forecasts, as shown by Fig. 7. As expected, the percent improvement is largest for non-rawinsonde initialization times, when it exceeds 10% at some levels. Particularly striking is the relatively small improvement at non-rawinsonde times between 250 and 350 mb. This is consistent with the large number of asynoptic aircraft observations at these levels, which leads to a decreased percent improvement for the lidar observations.

It is important to reiterate that all of these results represent the most optimistic scenario due to the use of error-free lidar observations and the neglect of cloud attenuation of the lidar beam. Nevertheless, they suggest that lidar observations do have the potential to significantly improve regional model skill scores. Additional experiments are under way to assess the degree of forecast improvement when realistic errors are added to the simulated lidar observations and realistic attenuation of the lidar beams by clouds is accounted for. Initial results from these tests have indicated that small (1 m s^{-1}) random errors cause little degradation in the percent improvement scores and that the impacts from clouds are confined mostly to levels below 850 mb. These results are likely too optimistic; however, because we have not added correlated errors. Correlated errors are quite likely for a satellite-borne observing platform and are more detrimental to model performance than random errors.

5. SUMMARY AND CONCLUSIONS

A series of regional OSSEs has been completed to evaluate the potential impact on forecasts from a Doppler wind lidar flown aboard a polar orbiting satellite. Idealized experiments designed to provide the most optimistic results indicate that improvements to regional forecast skill are realized through both the direct assimilation of lidar winds within the regional assimilation cycle and the use of lateral boundary conditions from a global model that has itself benefited from the assimilation of lidar winds. The two pathways exhibit opposite time tendencies; the percent improvement from regional assimilation decreases

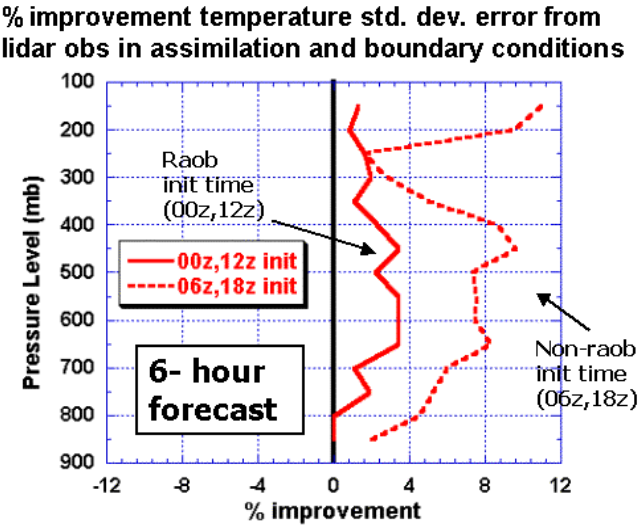

Fig. 7. Vertical profiles of percent improvement for 6-h temperature forecasts from combining assimilation of idealized lidar observations on the regional domain with the use of idealized lidar observations in the lateral boundary conditions (shown for rawinsonde and non-rawinsonde initialization times). Positive values shown indicate smaller std. dev. errors when the lidar observations are utilized.

with time while the percent improvement from the lateral boundary conditions increases with time. When both pathways are accounted for, the combined forecast improvement is nearly the sum of the two pathways and can exceed 12% for the non-rawinsonde initializations. As expected, the forecast improvement is most pronounced for the model predicted winds (compared to other model fields) and larger for non-rawinsonde initialization times (0600, 1800 UTC) than rawinsonde initialization times (0000 UTC, 1200 UTC). Based on the encouraging results obtained for the idealized regional lidar OSSE, we believe that further OSSE work on a space-based lidar wind profiling system is merited. In particular, additional simulation experiments should be conducted to refine the estimated forecast improvement for the more realistic case of lidar observations with errors and cloud attenuation.

6. ACKNOWLEDGMENTS

This work was supported by the National Oceanic and Atmospheric Administration. We would like to express our sincere appreciation to M. Masutani for providing considerable guidance on the lidar OSSE project in general and the use of the global model datasets in particular. We also appreciate the helpful discussions with S. Wood, J. Woollen, S. Greco, J. Terry, R. Atlas, and D. Emmitt. We acknowledge Paul Schultz and Susan Carsten for careful scientific and technical reviews, respectively.

7. References

Atlas, R., 1997: Atmospheric observations and experiments to assess their usefulness in data assimilation. *J. Meteor. Soc. Japan,* **75**, 111-130.

Baker, W. and coauthors, 1995: Lidar measured winds from space: a key component for weather and climate prediction. *Bull. Amer. Meteor. Soc.,* **76**, 869-888.

Barker, D. and Q. Zhang, 2001: Calibration of the MM5 nature run trajectory. http://www.mmm.ucar.edu/individual/barker/lidar_osse/results/calibration.html

Benjamin, S.G., G.A. Grell, J.A. Brown, T.G. Smirnova, and R. Bleck, 2003a: Mesoscale weather prediction with the RUC hybrid isentropic/terrain-following coordinate model. *Mon. Wea. Rev.,* **131**, in press.

Benjamin, S.G., D. Devenyi, S.S. Weygandt, K.J. Brundage, J.M. Brown, G.A. Grell, D. Kim, B.E. Schwartz, T.G. Smirnova, T.L. Smith, and G.S. Manikin, 2003b: An hourly assimilation/ forecast cycle: The RUC. *Mon. Wea. Rev.*, **131**, in press.

Devenyi, D., and S.G. Benjamin, 2003: A variational assimilation technique in a hybrid isentropic-sigma coordinate. *Meteor. Atmos. Phys.*, **82**, 245-257.

Feingold, G. M. Hardesty and B. Rye, 2002: Modeling observations from the wind-finding lidar. Report on Regional OSSE, ETL contribution. 17 pp.

Grell, G., and D. Devenyi, 2002: A generalized approach to parameterizing convection combining ensemble and data assimilation techniques. *Geophys. Res. Let.* **29**, 38-1-4.

Lord, S.J., E. Kalnay, R. Daley, G.D. Emmitt, R. Atlas, 1997: Using OSSEs in the design of future generation integrated observing systems. Preprints, *1st Symp. On Integrated Observing Systems.* Long Beach, CA, AMS.

Lord, S.J. and coauthors, 2001: Observing System Simulation Experiments for NPOESS. Preprints, *5th Symp. On Integrated Observing Systems.* Albuquerque, NM, AMS, 168-173.

Lord, S.J. and coauthors, 2002: Impact assessment of a Doppler wind lidar for NPOESS/OSSE. Preprints, *6th Symp. On Integrated Observing Systems.* Orlando, FL, AMS, 108-115.

Marroquin, A., J.R. Smart, and L.S. Wharton, 2001: Considerations in providing a natural dataset for lidar OSSE studies. Preprints, *14th Conf. on Num. Wea. Pred.* Ft. Lauderdale, FL, AMS, 306-309.

Masutani, M. and coauthors, 2002: Calibration and error sensitivity tests for NPOESS/OSSE. Preprints, *6th Symp. On Integrated Observing Systems.* Orlando, FL, AMS, 71-76.

Smirnova, T.G., J.M. Brown, S.G. Benjamin, and D. Kim, 2000: Parameterization of cold-season processes in the MAPS land-surface scheme. *J. Geophys. Res.*, **105**, D3, 4077-4086.